Investigating the Low Temperature Formation of CuII-(N,O) Species on Cu-CHA Zeolites for the Selective Catalytic Reduction of NOx

(Article begins on next page)

24 December 2024

Investigating the low temperature formation of Cu(II)-(N,O) species on Cu-CHA zeolites for the Selective Catalytic Reduction of NOx

Chiara Negri,[a] Peter S. Hammershøi,[b][c] Ton V.W. Janssens,[b] Pablo Beato,[d] Gloria Berlier,*[a] and Silvia Bordiga*[a]

Abstract

In this work, we show the potentiality of *operando* FTIR spectroscopy to follow the formation of Cu^{II}–(N,O) species on Cu exchanged chabazite zeolites (Cu-CHA), active for the selective catalytic reduction of NO_x with NH_3 (NH_3-SCR). In particular, we investigated the reaction of NO and O_2 at low temperature (200 and 50 °C) on a series of Cu-CHA zeolites with different composition (Si/Al and Cu/Al ratios), to investigate the nature of the formed copper nitrates, which have been proposed to be key intermediates in the oxidation part of the SCR cycle. Our results show that chelating bidentate nitrates are the main structures formed at 200 °C. At lower temperature a mixture of chelating and monodentate nitrates are formed, together with the nitrosonium ion NO^+., whose amount was found to be proportional to the zeolites Brønsted sites concentration. Nitrates were found to mainly form with Cu^{II} ions stabilized by one negative framework charge (Z), Z-[Cu(OH)]^I or Z-[Cu(O$_2$)]^I, without involvement of Z_2-Cu^{II} ones. This evidence, together with the absence of bridging nitrates in samples with high probability for Cu-Cu pairs, indicate that the nitrate ligands are not able to mobilize copper ions, at variance with what recently reported for NH_3. Finally, water was found to replace preformed chelating copper nitrates and deplete NO^+ (though with different kinetics) at both temperatures, while favouring the presence of monodentate ones.

[a]   C. Negri, Dr. G. Berlier and Prof. S. Bordiga
        Department of Chemistry, INSTM Reference Center and NIS Interdepartmental Center
        University of Turin
        Address Via Giuria 7, I-10135 Turin, Italy
        E-mail: gloria.berlier@unito.it, silvia.bordiga@unito.it
[b]   P.S. Hammershøi, Dr. T.V.W. Janssens
        Umicore Denmark ApS
        Nøjsomhedsvej 20, 2800 Kgs. Lyngby, Denmark
[c]   P.S. Hammershøi
        Department of Chemical and Biochemical Engineering
        Technical University of Denmark,
        Lyngby, Denmark
[d]   Dr. P. Beato
        Haldor Topsøe
        Kgs. Lyngby 2800, Denmark

Introduction

As a consequence of their outstanding performance in the selective catalytic reduction (SCR) of NO_x with NH_3, copper ion-exchanged chabazite zeolites (Cu-CHA) have been studied intensively over the last decade.[1] More recently, they have also been proofed to be active in the low temperature activation of methane to its direct transformation to methanol.[2] The catalytic activity of Cu-CHA materials is due to the copper ions, which compensate the negative charge on the zeolite framework induced by the presence of Al heteroatoms. These copper ions reversibly can change the oxidation state between Cu^{II} and Cu^{I} depending and form a number of different species inside the zeolite, depending on the activation atmosphere,[3] and can therefore act as active sites for redox reactions.

The NH_3-SCR reaction is the basis of the current technology for the abatement of NO_x emissions from diesel engines, and involves the reaction of NO with NH_3 in the presence of O_2 according to the equation:

$$4\ NH_3 + 4\ NO + O_2 \rightarrow 4\ N_2 + 6\ H_2O \qquad (1)$$

The NH_3-SCR reaction cycle consists of an oxidation and a reduction part.[4] The oxidation part involves oxidation of a Cu^{I} species to Cu^{II} under the influence of $NO + O_2$, and the reduction part is the reduction of the Cu^{II} species to Cu^{I} by a mixture of $NH_3 + NO$. The NH_3-SCR reaction can be executed by alternating these oxidation and reduction steps. The reduction leads to the formation of a $Cu^{I}(NH_3)_2$ complex, which is weakly bound to the zeolite and therefore is mobile.[4b, 4c, 5] The oxidation of this $Cu^{I}(NH_3)_2$ complex with $NO + O_2$ results in the formation of a $Cu^{II}NO_3^-$ species.[4b, 6]

An important and difficult step in the NH_3-SCR reaction is the dissociation of oxygen. DFT calculations have shown that oxygen dissociation becomes easier when it proceeds over a pair of Cu-ions, and the presence of NO further enhances this dissociation.[4b, 7] It is clear that the propensity for Cu pair formation increases with the Cu loading, as the average distance between the Cu-ions diminishes. Since the Cu ions require 1 or 2 Al atoms in the zeolite framework, the Si/Al ratio must be sufficiently low in order to obtain a high enough Cu loading in the CHA zeolite for Cu-pair formation. Apart from the Si/Al ratio, the distribution of the Al-atoms in the zeolite framework is important as well, as Cu-pair formation is less likely to occur in the vicinity of 2 Al atoms that are located close together.[8]

What is known about Cu speciation in Cu-CHA, is that after activation in O_2 Cu^{II} ions can be present as Z-[Cu(OH)]^{I} (requiring only one vicinal framework Al for charge compensation, denoted as Z) and/or as Z_2-Cu^{II}, stabilized by two framework negative charges. The relative fraction of these two families of sites in 8 and 6-members rings of the chabazite cage (8r and 6r), was shown to be a function of the Si/Al and Cu/Al ratios of the zeolite.[3, 4c, 9] The evidence for the presence of [Cu(OH)]^{I} sites is based on FTIR and X-ray absorption (XAS) spectroscopies.[3, 10] In particular, EXFAS data refinement for these sites is in agreement with the presence of tri-coordinated Cu^{II}, linked to two framework oxygen atoms and to one from the OH$^-$ ligand. More recently, high resolution high energy resolution fluorescence detected XAS experiments in the near-edge region (HERFD XANES), indicated that in O_2-activated Cu-CHA a fraction of the Cu^{II} ions stabilized by one framework negative charge could have a similar tri-coordinated geometry when bonding a superoxo ligand, resulting in [Cu(O$_2$)]^{I} sites,[11] as also evidenced by Raman experiments.[2b]

Recently, it has been shown that the mobility of the $Cu^{I}(NH_3)_2$ complexes plays an important role for the formation of Cu pairs as well (and consequent oxygen activation),[4c] and that this actually is the reason for the high activity of Cu-CHA catalysts for NH_3-SCR at low temperatures. The often observed decrease in NO_x conversion with increasing temperatures is then ascribed to a loss of mobility of the Cu ions, as the $Cu^{I}(NH_3)_2$ complex decomposes.[6a, 12]

The formation of $Cu^{II}NO_3^-$ species is generally observed upon exposure of a Cu-CHA catalyst to a mixture of NO and O_2.[4b, 6a, 12a, 13] It is generally accepted that in the presence of both NO and O_2 in

the gas phase N_2O_3 and N_2O_4 can readily form. The formation of NO_3^- can be explained by the disproportionation of N_2O_4, forming NO^+ and NO_3^-. Interested readers can refer to recent experimental[13b] or computational works[7b] about mechanistic insights. Even though $Cu^{II}NO_3^-$ species are detected spectroscopically after oxidation of Cu-CHA in NO and O_2, the role of these NO_3^- species in NH$_3$-SCR is not clear yet. In the mechanism proposed by Janssens et al., the nitrate species are a part of the SCR cycle, and are in equilibrium with a $Cu^{II}NO_2^-$ species.[4b, 14] In situ XAS measurements have not revealed nitrate species under typical conditions for NH$_3$-SCR,[6a] which means that nitrates are not an intermediate or that their steady state concentration is below the detection level. The fact that $Cu^{II}NO_3^-$ species can be reduced with a mixture of NH$_3$ and NO to the Cu^I(NH$_3$)$_2$ complex,[4b, 4d, 6] and that the $Cu^{II}NO_3^-$ species is rather stable and often detected experimentally actually points to $Cu^{II}NO_3^-$ as an intermediate for the NH$_3$-SCR reaction as well.

On the other hand, the role of key Cu^{II}(N,O) intermediates was debated by Chen et al., suggesting the relevance of the nitrosonium ion NO$^+$ (formed in higher amount on Cu-CHA with respect to Cu-BEA zeolites).[15] Similarly, Ruggeri et al. proposed NO$^+$ (with formal oxidation state of +3, thus considered as a 'nitrite-like' specie), to be an intermediate in the stepwise oxidation of NO (+2) to NO$_2$ (+4), involving Cu dimers in Cu-CHA.[13b] Moreover, the mechanism explaining the effect of NO$_2$ in the flow on SCR rate (fast SCR, eq. 2), still deserves further investigation, notwithstanding the interesting micro-kinetic analysis by Colombo et. al.[4b, 4c, 13c]

$$4\ NH_3 + 2\ NO + 2\ NO_2 \rightarrow 4\ N_2 + 6\ H_2O \qquad (2)$$
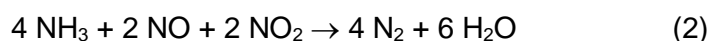
To obtain more insight in the formation and reactivity of the Cu^{II}-(N,O) species that is formed by oxidation in a mixture of NO and O$_2$, we present the results obtained using FTIR spectroscopy in *operando* conditions on a series of Cu-CHA zeolites with different composition, investigating the effect of temperature (200 *vs* 50 °C) and of water presence in the flow. The low temperature reaction regime is of interest for vehicles during their cold start transients[13c] and the effect of water is important, since it is always present in the exhaust gas effluents.[13b] Finally, comparison of the results obtained on samples with different compositions allowed us to propose an interpretation of the complex nitrate spectra often observed in zeolites, with implications about the mobility of Cu ions in the presence of nitrate ligands. These findings should shed some light into the debate concerning the NO$^+$ and $Cu^{II}NO_3^-$ intermediates in NH$_3$-SCR, with the caveat that we are not dealing yet with the reactivity of adsorbed Cu^{II}-(N,O) species with NH$_3$.

Results and discussion

The reaction of NO and O$_2$ with Cu-CHA was studied on four samples with different Si/Al and Cu/Al ratios by operando FTIR spectroscopy at 200 °C and 50 °C, in dry and wet (5% H$_2$O) conditions. We will first focus on the effect of the temperature and presence of water vapour on a sample with Si/Al = 15, Cu/Al = 0.5 (CHA15_05), and then move to discuss the effects of the Si/Al and Cu content on the structure of the formed Cu^{II}-(N,O) species. In all cases, the samples were pre-treated in pure O$_2$ at 400 °C for 1 h. After this treatment a mixture of Z-[Cu(OH)]^I and Z$_2$-Cu^{II} ions is present, depending on the samples composition.[3] [6b, 9] Table 1 summarizes the chemical composition of the four samples, and the expected relative fraction of Z-[Cu(OH)]^I and Z$_2$-Cu^{II} sites, on the basis of the compositional phase diagram proposed by Paolucci et al.[6b]

Table 1 Chemical composition of the studied sample and predicted fraction of Z-[Cu(OH)]^I and Z$_2$-Cu^{II} sites[6b]

Sample	Si/Al	Cu/Al	Cu wt%	Z-[Cu(OH)]^I	Z$_2$-Cu^{II}
CHA15_05	15	0.5	2.6	0.7 − 0.8	0.2 − 0.3

CHA15_02	15	0.2	1.3	~ 0.5	~ 0.5
CHA5_01	5	0.1	1.5	0	1
CHA29_06	29	0.6	1.7	0.9 - 1	0 – 0.1

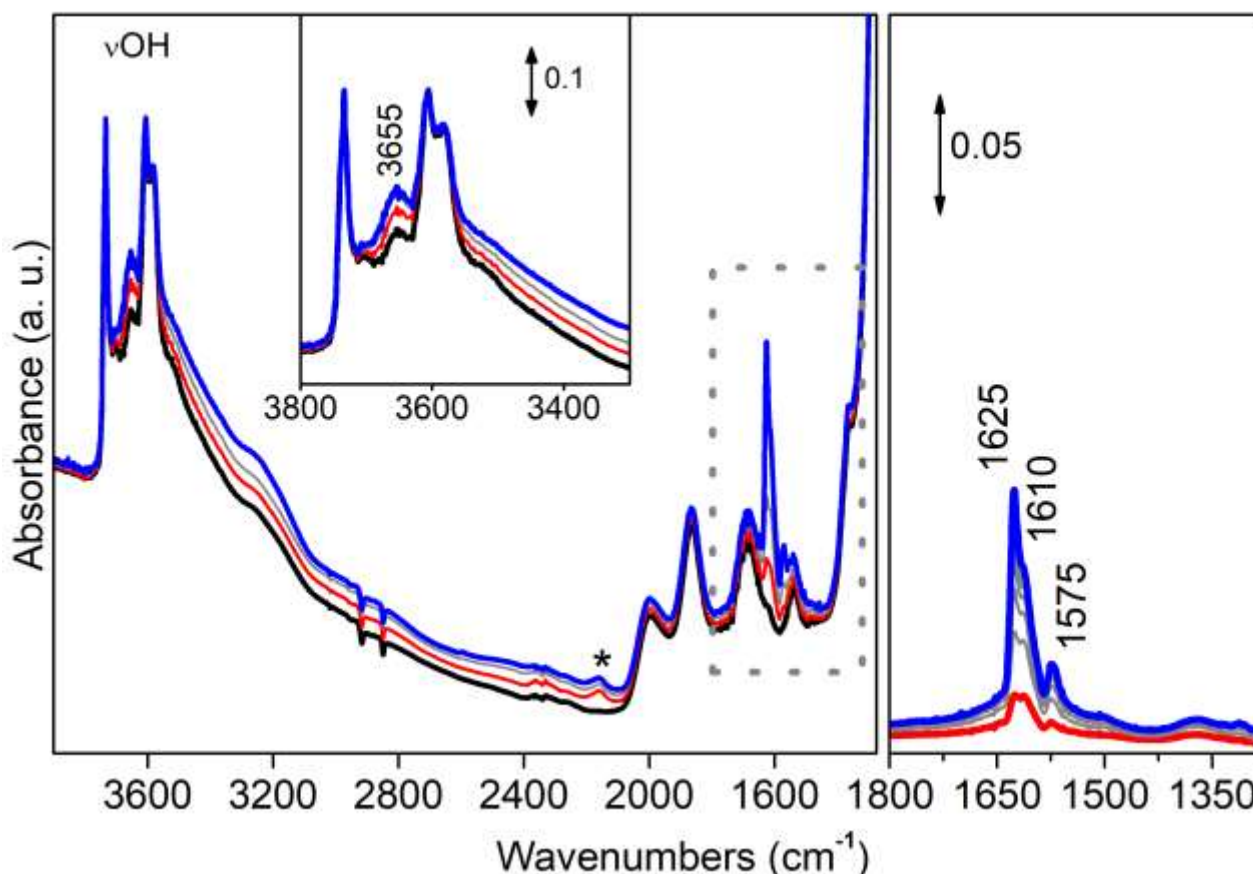**Effect of temperature on the NO/O₂ reactivity on Cu-CHA**

Figure 1. FTIR spectra measured during exposure of Cu-CHA (Si/Al = 15, Cu/Al 0.5, 2.6 wt% Cu) to 1000 ppm NO / 10% O_2 at 200°C. Black curve: after pre-treatment in pure O_2 at 400 °C for 1 h; red curve: after NO/O_2 admission; blue curve: after 30 minutes; grey curves: intermediate times of contact. Magnifications of the νOH regions and of the Cu^{II}-(N,O) regions (dotted grey box in left panel) are reported in the inset and in right hand panel, respectively. The spectra for the Cu^{II}-(N,O) region were corrected for the background by subtraction of the spectrum for the zeolite before NO/O_2 admission. See text for meaning of the * and # symbols.

Figure 1 shows the development of the FTIR spectra in the range 3900-1300 cm^{-1} for CHA15_05 in a NO/O_2 flow at 200 °C. The sample was cooled to 200 °C in pure O_2 (black curve) to maintain the Cu^{II} state before admitting the NO/O_2 mixture. The starting material is characterized by the typical signals in the OH stretching region (νOH, 3800 – 3300 cm^{-1}), and by the overtone and combination framework modes in the 2100 – 1300 cm^{-1} interval. The lower frequencies (not shown) are dominated by the intense zeolite framework modes.

The four main bands the in νOH region are at 3732 (isolated Si-OH), 3604 and 3582 (CHA Brønsted sites) and 3655 cm^{-1}, assigned to the νOH mode of the Z-[Cu(OH)]^{I} site.[10] The presence of the intense signals due to Si(OH)Al Brønsted sites indicates that not all available Brønsted sites are

5

exchanged with Cu, which is consistent with the Cu/Al ratio of about 0.5. The region between 2100 and 1300 cm^{-1} is characterized by the typical overtone and combination modes of the TO$_4$ zeolite framework vibrations (T representing a Si or Al framework atom), at 1998, 1868, 1682 and 1542 cm^{-1}.

Contacting the zeolite with a 1000 ppmNO/ 10% O$_2$ mixture at 200 °C (red, grey and blue curves), results in changes in the νOH and overtone/combination regions, and the development of a very weak band at 2159 cm^{-1} labeled with *.Furthermore, there is a slight vertical shift of the background zeolite spectrum. The band at 3655 cm^{-1} grows and reaches a steady state after 3 minutes in NO/O$_2$ (see inset of Figure 1). In the range 1800-1300 cm^{-1}, three sharp peaks at 1625, 1610 (shoulder) and 1575 cm^{-1} appear, which have been assigned to $Cu^{II}NO_3^-$ species (1625, 1610 and 1575 cm^{-1}).[4b, 13b, 14-15] The weak band at 2159 cm^{-1} indicates the formation of the nitrosonium NO$^+$ ion exchanging Brønsted sites (see below).[15-16] The very weak signal at 1380 cm^{-1} (labelled with # in right hand panel) is related to the formation of a very small amount of water molecules, hydrogen bonded to the Brønsted sites, which are also responsible for the growth of the band at 3655 cm^{-1} (see below).

A number of significant changes in the FTIR spectrum are observed, when the temperature of NO/O$_2$ exposure is lowered to 50 °C (Figure 2). The spectrum measured after heating in O$_2$ at 400 °C and subsequent cooling in O$_2$ to 50 °C (black curve) is similar to the one measured at 200 °C, and no traces of water contamination are observed. This indicates that the Cu-CHA material itself is not affected by the lower temperature. However, the changes observed upon exposure to 1000 ppm NO/10% O2 at 50 °C are different and more pronounced, compared to those observed at 200 °C. First, the bands at 3670 cm^{-1} and 3544 cm^{-1} in the νOH region continue to grow with the parallel consumption of the Brønsted signals (see inset). Secondly, broad signals centred at 2884, 2416 and 1670 cm^{-1} appear, labelled as A, B and C. Third, the band at 2159 cm^{-1} (labelled with *) grows in the first minutes (green curve) to a clearly visible intensity, after which it decreases again. Fourth, the three bands at 1625, 1610 and 1575 cm^{-1} (magnified in the right hand panel) show a gradual increase with time, with a final intensity significantly higher compared to those observed at 200 °C. Finally, some weaker bands are also observed at 1500, 1380 (labelled with #) and 1310 cm^{-1}.
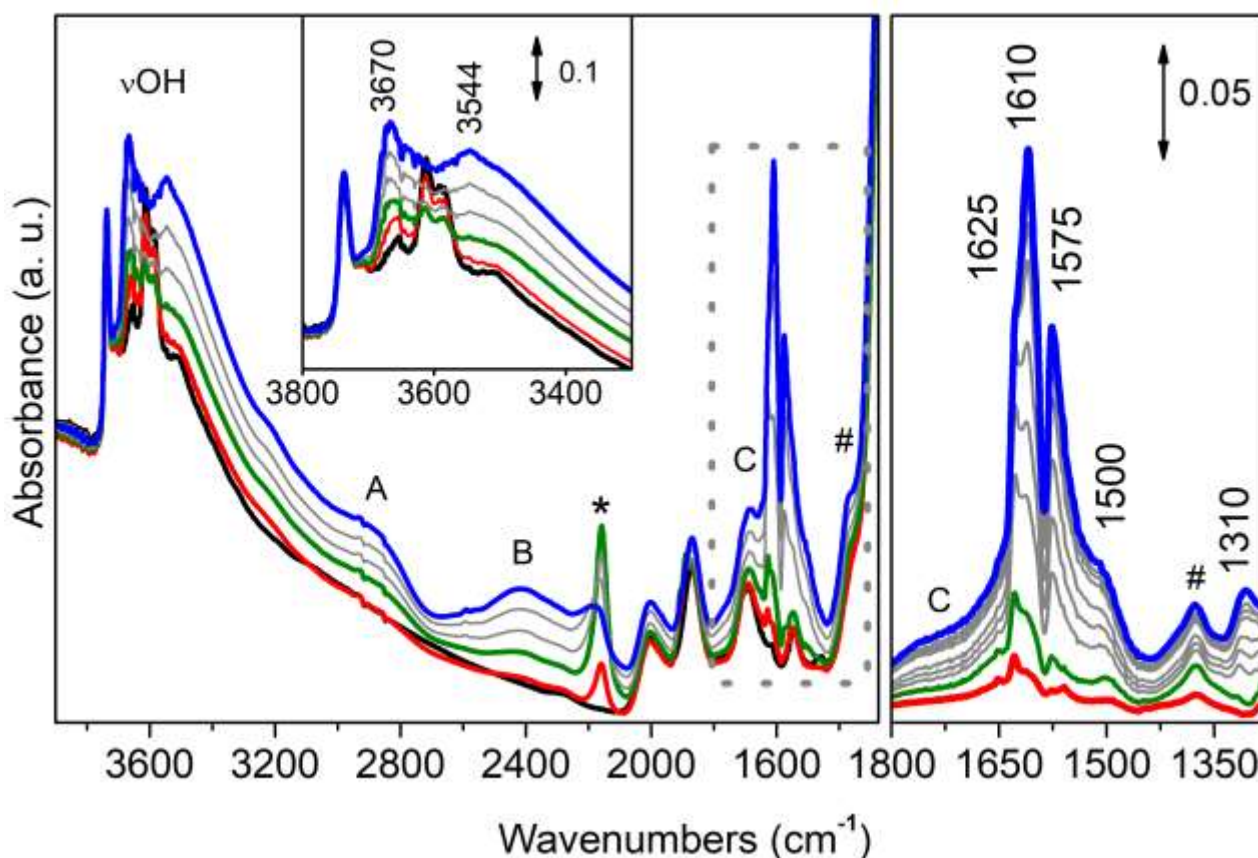
Figure 2. FTIR spectra measured during exposure of Cu-CHA (Si/Al = 15, Cu/Al 0.5, 2.6 wt% Cu) to 1000 ppm NO / 10% O_2 at 50°C after pre-treatment in O_2 (black curve), after NO/O_2 admission (red), after 2 and 30 minutes (green and blue). Intermediates spectra in grey. Magnifications of the νOH regions and of the Cu^{II}-(N,O) regions (dotted grey box in left panel) are reported in the inset and in right hand panel, respectively. The spectra for the Cu^{II}-(N,O) region were corrected for the background by subtraction of the spectrum for the zeolite before NO/O_2 admission.

The main differences between the experiments carried out at 200 and 50 °C can be summarized as follows. First, the changes in the νOH region, the broad bands labelled as A, B and C and the band at 1380 cm^{-1} (labelled with #) are all typical fingerprints of highly perturbed OH groups involved in strong hydrogen bond, formed by interaction of water molecules with the zeolites Si(OH)Al Brønsted sites.[17] Water molecules are formed by reaction of NO in the presence of O_2 and H$^+$ Brønsted sites to form the NO$^+$ ions (band at 2159 cm^{-1}, labelled with *), which are replacing the reacted Brønsted sites.[15-16, 18] Our results thus indicate that NO$^+$, if formed at 200 °C, either is not stable and further reacts, or is in competition with other reactions.

The *ABC* triplet arises from a Fermi resonance of the νOH mode in ($_{zeolite}$O-H…O$_{water}$) complexes (labelled as (a) in Scheme 1, with the overtone of the in-plane bending mode (2δ($_{zeolite}$O-H….O$_{water}$)) giving the *AB* diad and the overtone of the out-of-plane bending mode (2δ($_{zeolite}$O-H….O$_{water}$)) giving the *C* band. In the *B* band, the stretch is also coupled with the second overtone of the out-of plane bending. The additional bands around 3670 and 3544 cm^{-1}are assigned to νOH modes of slightly perturbed H_2O molecules (labelled as (b) and (c) in Scheme 1). This indicates that in the tested conditions ($H_2O)_n$/H$^+$ adducts are formed, with $n \leq 1$. Notice that the same features (though much weaker, in agreement with the lower intensity of the NO$^+$ band) are observed at 200 °C.

7
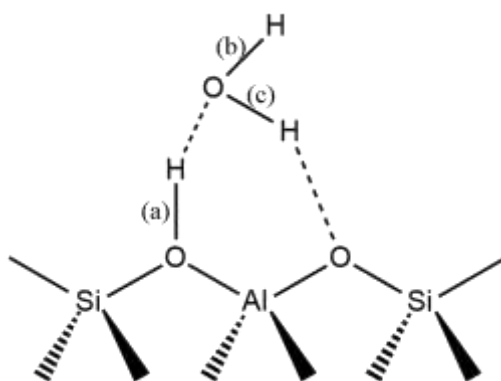
Scheme 1 Schematic representation of a zeolite Brønsted site involved in a strong hydrogen bond with an H_2O molecule

The comparison of the changes at 1625, 1610 and 1575 cm^{-1} observed by exposure to NO/O$_2$ at 50°C and 200 °C provides further information on the properties and structure of the formed $Cu^{II}NO_3^-$ species. The three bands at 1625, 1610 and 1575 cm^{-1} have been previously assigned to chelating bidentate structures, involving one Cu^{II} ion (Scheme 2, left).[4b, 14] However, the data in Figure 2 show that the intensity ratio 1625/1610 cm^{-1} is high in the beginning, but gradually decreases. This points to the presence of more than one chelating nitrate (see below for details about assignment), whose relative concentration depends upon temperature. Moreover, a third species is formed at 50 °C, which is virtually absent at 200 °C (bands at 1500 and 1310 cm^{-1}). On the basis of their position (see below) these are assigned to monodentate $Cu^{II}NO_3^-$ complexes, with low thermal stability (right structure in Scheme 2).

Scheme 2. Pictorial representation of the structure of different $Cu^{II}NO_3^-$ complexes involving Cu^{II} ions in the chabazite 8-member ring: chelating bidentate (left), bridging bidentate (middle) and monodentate (right). Cu: green, Si: white, Al: yellow, O: red and N: blue. The labels ν$_{NO2}$ and ν$_{N=O}$ indicate the corresponding vibrational modes observed and discussed in this work.

Thus, lowering the reaction temperature increases the overall amount of adsorbed nitrates (compare the overall bands intensity in Figures 1 and 2) and influences their speciation: monodentate nitrates are present together with a sensibly higher amount of at least two distinct chelating ones. This observation is in agreement with the relatively low thermal stability of nitrates (in the order monodentate < bidentate) and suggests that at 200 °C not all Cu^{II} ions are involved in nitrate formation.

The different thermal stability of the different Cu^{II}-(N,O) species observed at 50 °C is further illustrated by a continuous measurement of the FTIR spectra in an atmosphere of 1000 ppm NO/10% O$_2$ during cooling from 200 °C to 50 °C. These data are shown in Figure 3. With decreasing temperature, a general broadening of the spectra is observed, as a consequence of the formation of strongly perturbed hydroxyls groups (Scheme 1), with fingerprints around 1670 and 1380 cm^{-1}

(labelled as C and #). The gradual growing of these features is accompanied in the whole range (see Fig S1 in SI) by the corresponding evolution of the (b) and (c) νOH groups (3670 and 3544 cm^{-1}, Scheme 1) and AB diad, and by that of NO+ (* feature at 2159 cm^{-1}). The final state is very similar to that obtained after 30 minutes in NO/O$_2$ flow at 50 °C (Figure 2), including the formation of monodentate nitrates with bands at 1500 and 1301 cm^{-1}. The interesting point is that the intensity at 1625 cm^{-1} reaches a maximum around 80 °C after which it decreases slightly, while the peaks at 1610 and 1575 cm^{-1} continue to grow, resulting in the lower relative intensity for I(1625)/I(1610). This indicates that the peak at 1625 cm^{-1} and those at 1610 and 1575 belong to different Cu^{II}-(N,O) species, and that the less stable species is favoured at temperatures below 80 °C.

To get further insights into the possible correlations between the different Cu^{II}-(N,O) species (*i.e.* bidentate and monodentate nitrates, NO$^+$) we carried out an analysis of the different components intensity. The corresponding plots clearly show a no correlation between the decrease of the band at 1625 cm^{-1} and the growth of neither monodentate nitrates nor NO$^+$ (SI, Fig S2).
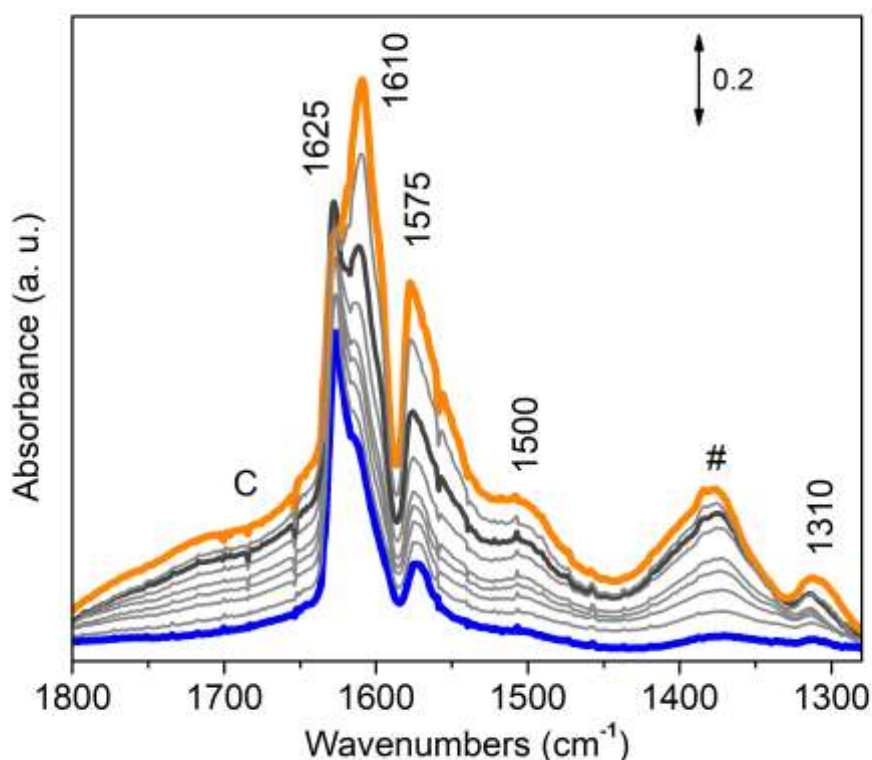

Figure 3. FTIR spectra measured during exposure of Cu-CHA (Si/Al = 15, Cu/Al 0.5, 2.6 wt% Cu) to 1000 ppm NO / 10% O$_2$ after pre-treatment in O$_2$, while decreasing temperature from 200 (blue curve) to 50°C (orange curve). Intermediate temperature are in grey, the dark grey curve corresponds to the highest intensity reached by the 1625 cm^{-1} component before decreasing (80 °C). Spectra were corrected for the background by subtraction of the spectrum for the zeolite at 200 °C before NO/O$_2$ admission.

Effect of water on the NO/O$_2$ reactivity on Cu-CHA

The reactivity of the NO/O$_2$ mixture on Cu-CHA zeolites was studied in the presence of water, which is usually present in the SCR flow. Thus, 5% of H$_2$O was added to the NO/O$_2$ flow on CHA15_05

previously saturated with Cu^{II}-(N,O) species (that is after 30 minutes in dry NO/O_2 flow): the obtained spectra are reported in Figures 4 and 5 at the two studied temperatures. A similar set of experiments was carried out by directly dosing on the zeolite pre-activated in O_2 a NO/O_2/H_2O flow, with similar results (see Figures S3 and S4 in SI).

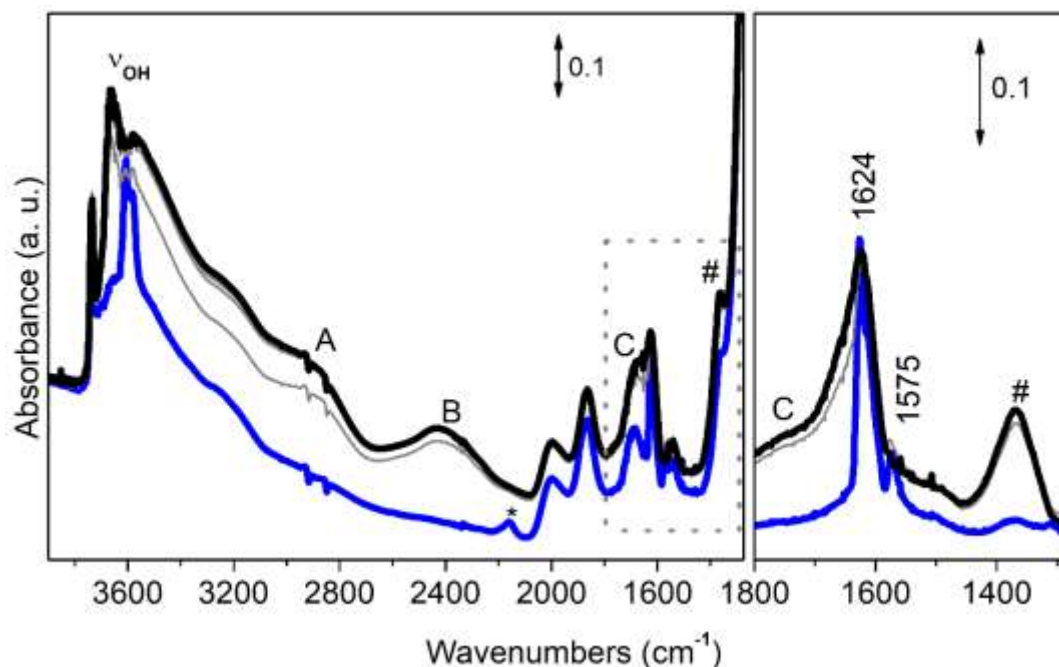Figure 4. FTIR spectra measured during exposure of Cu-CHA (Si/Al = 15, Cu/Al 0.5, 2.6 wt% Cu) to 1000 ppm NO/10% O_2/5% H_2O at 200°C after saturation of surface with nitrates. Starting point (blue), under wet flow (grey), after 30 min (black). The spectra magnified in the Cu^{II}-(N,O) region (right) were corrected for the background by subtraction of the spectrum for the zeolite before NO/O_2 admission.

In the experiment performed at 200°C (Figure 4) the addition of water to the feed causes an immediate change in the nitrate region, with very small changes as a function of time; grey and black curves were collected at 5 and 30 minutes respectively. The bending mode of water (δH_2O, maximum at 1624 cm^{-1}) shows a strong asymmetry towards the high frequency side, testifying the co-presence of physisorbed and hydrogen bonded water. The typical fingerprints of strongly perturbed hydroxyl groups (ABC and # bands) indicates that in these conditions only 1:1 H_2O/H^+ adducts are present (Scheme 1). Thus, the typical δH_2O mode at 1624 cm^{-1} is related to water molecules physisorbed on Cu^{II} ions, replacing the previously formed nitrates. Indeed, only the component at 1575 cm^{-1} is distinguishable in the first spectrum under wet conditions, and then disappear. On the other hand, NO$^+$ disappears immediately, confirming an independent reactivity with respect to $Cu^{II}NO_3^-$.

When the same experiment is carried out at 50°C (Figure 5) we observe a different dynamic. Namely, in the first spectrum measured under wet flow, the typical fingerprints of hydroxyl groups involved in strong hydrogen bond are present (ABC triplet and #, corresponding to the 1:1 H_2O/H^+ adduct exemplified in Scheme 1). In these conditions NO$^+$ decreases, monodentate nitrates increase and chelating ones are not affected. After 2 min in wet flow (green curve) the hydrogen-bonded 1:1 H_2O/H^+ adduct is eroded as clusters of H_2O are formed, with consequent zeolite deprotonation and formation of nH_2O/H^+ adducts (n $\geq$ 1) (Scheme 3). This is testified by the disappearance of the ABC triplet and # feature, and by the broad absorption in the 3700 – 2400 cm^{-1} range, typical of hydrogen bonded water clusters, which are also involving surface silanols.

Scheme 3 Evolution of hydrogen bonded 1:1 H_2O/H^+ adducts into nH_2O/H^+ with n > 1, implying deprotonation and presence of H_2O clusters

Under these conditions, NO^+ is totally depleted (*), monodentate nitrates (1500 and 1310 cm^{-1}) rapidly increase reaching a steady state, and chelating nitrates are replaced by physisorbed water (see band at 1575 and δH_2O at 1624 cm^{-1}). New features are observed, gradually growing under the wet flow (1425 and 1344 cm^{-1}) which have been assigned to solvated nitrates ions.[19]
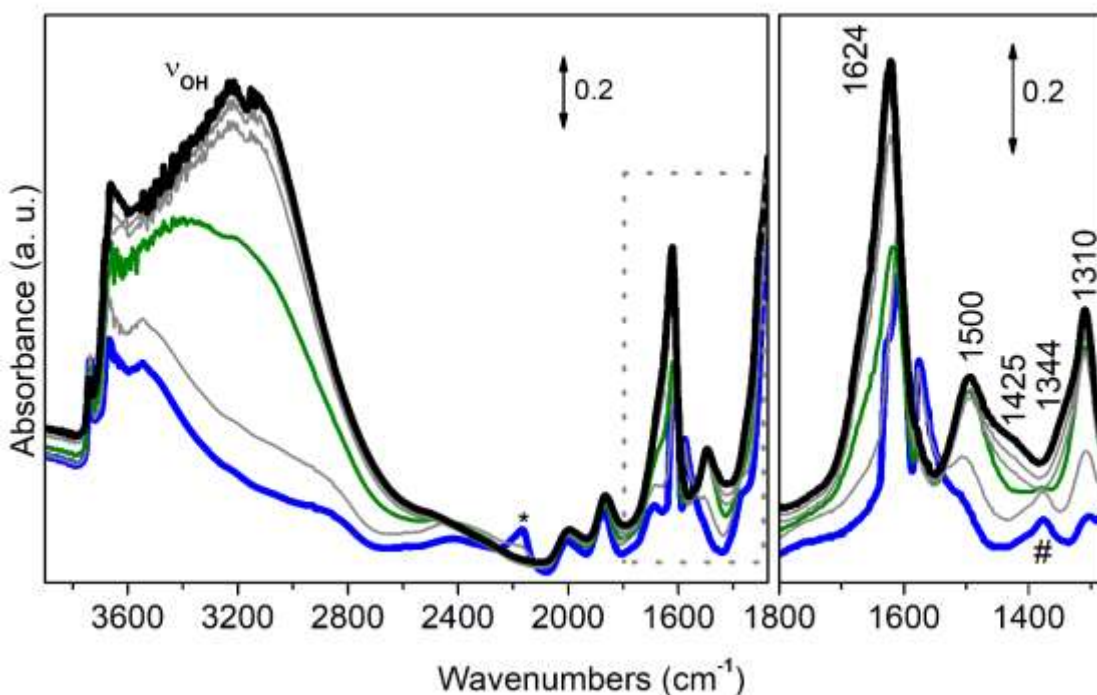
Figure 5. FTIR spectra measured during exposure of Cu-CHA (Si/Al = 15, Cu/Al 0.5, 2.6 wt% Cu) to 1000 ppm NO/10% O_2/5% H_2O at 50°C after saturation of surface with nitrates (blue). Spectra measured under wet flow are in grey, after 2 and 30 min in green and black, respectively. The spectra magnified in the Cu^{II}-(N,O) region (right) were corrected for the background by subtraction of the spectrum for the zeolite before NO/O_2 admission.

Effect of Cu-CHA composition on formed Cu^{II}-(N,O) species

Figure 6. FTIR spectra measured after 30 minutes exposure of Cu-CHA zeolites with different composition to 1000 ppm NO / 10% O_2 at 200°C after pre-treatment in O_2: *CHA15_05* (*red,* Si/Al = 15, Cu/Al 0.5,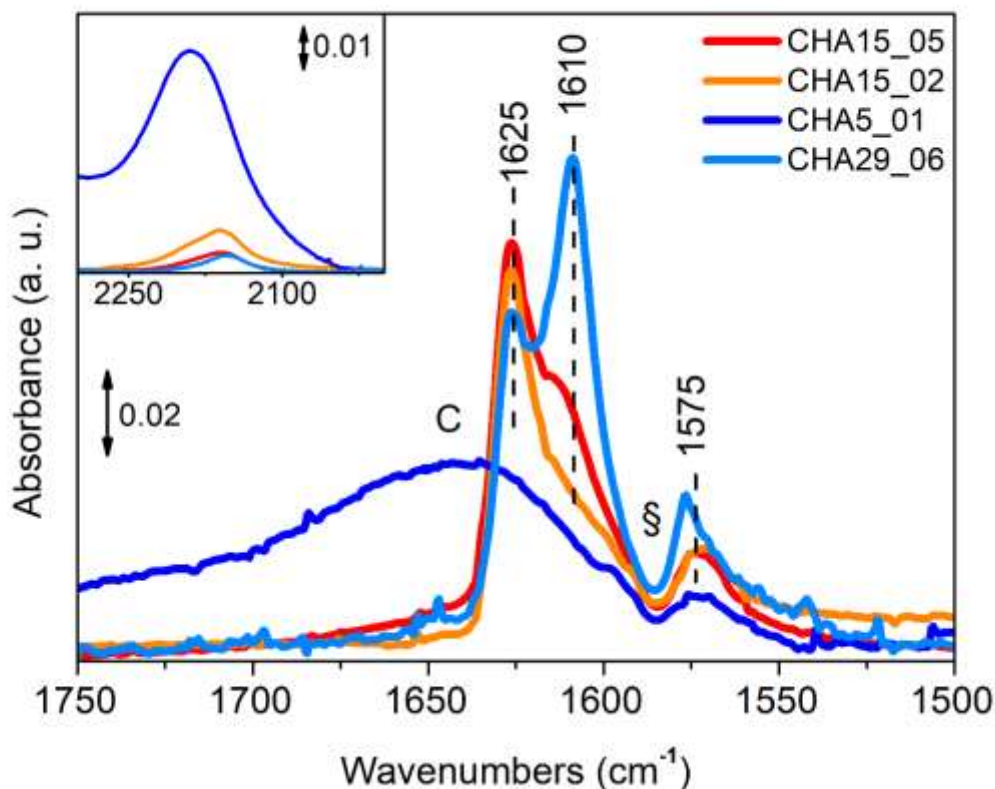 2.6 wt% Cu)*; CuCHA15_02* (*orange,* Si/Al = 15, Cu/Al 0.2, 1.3 wt% Cu)*; CuCHA15_05* (*blue, Si/Al = 5*, Cu/Al 0.1, 1.5 wt% Cu)*; CuCHA29_06* (*azure,* Si/Al = 29, Cu/Al 0.6, 1.7 wt% Cu). Spectra were corrected for the background by subtraction of the spectrum for the zeolite before NO/O_2 admission and normalized with respect to pellet thickness and Cu loading. The inset shows the corresponding NO^+ region.

The same set of experiments discussed above for CHA15_05 (Si/Al = 15, Cu/Al 0.5, 2.6 wt% Cu) has been carried out on the series of samples listed in Table 1, characterized by different Si/Al and Cu/Al composition. In this section we are comparing the results obtained in NO/O_2 flow at 200°C. To directly compare the data obtained after 30 minutes of NO/O_2 exposure, each spectrum has been normalized with respect to pellet thickness and Cu wt%. They are only reported in the spectral region of bidentate $Cu^{II}NO_3^-$ species (Figure 6), since for most of the samples these are the main bands formed in dry conditions at 200 °C (see Figures S5-S8 in SI for whole ranges). An exception is given by sample CHA5_01 (Si/Al = 5, Cu/Al 0.1, 1.5 wt% Cu), which is characterized by the formation of a relatively large amount of NO^+ (inset of Figure 6) and 1:1 H_2O/H^+ adducts (C component in Figure 6). A definitely smaller amount of NO^+ is also observed in the other samples, in the order CHA5_01 >>> CHA15_02 > CHA15_05 > CHA29_06. This trend nicely correlates with the amount of Brønsted sites in the different zeolites, in agreement with the mechanism proposed by Hadjiivanov et al.,[16a] further confirmed by Henriques et al. who studied NO^+ formation on (transition metal free) H^+ and Na^+ exchanged mordenite.[16b]

Apart from sample CHA5_01, the three peaks at 1625, 1610 and 1575 cm^{-1} described above are present in all samples, but significant differences can be seen in their relative intensity. More in detail, the peak at 1625cm^{-1} is most intense for CHA15_05, it progressively decreases from CHA15_02 to CHA29_06 and is virtually absent in CHA5_01. This trend is reversed for the two bands at 1610 and 1575 cm^{-1}, which reach highest intensities for CHA29_06, the zeolite with the highest Si/Al ratio Si/Al

= 29, Cu/Al 0.6, 1.7 wt% Cu). The observed evolution of bands further supports the interpretation given above, pointing the presence of more than one family of bidentate $Cu^{II}NO_3^-$ (left structure in Scheme 2) whose relative concentration is not only affected by temperature but also by Cu (and Brønsted) distribution and concentration.

Interpretation of the $Cu^{II}NO_3^-$ bands

This section aims at giving an interpretation of the bands generally assigned to bidentate nitrates, trying to rationalize the differences observed as a function of temperature and zeolite composition. For this purpose, a short review of the literature assignment is first discussed.

Generally, surface nitrates have a C$_{2v}$ symmetry (Scheme 2), resulting in three IR active stretching modes whatever configuration one assumes.[20] Monodentate structures only presents single N-O bonds, one connected to the Cu^{II} ion (N-O) and two equivalent ones (O-N-O) (right hand structure in Scheme 2). The bands at 1500 and 1310 cm^{-1}, observed at 50 °C in both dry and wet conditions coincide well with the reported v_{asNO2} and v_{symNO2} modes of monodentate nitrates, respectively, while the corresponding v_{N-O} falls in the lower energy region, which is covered by the zeolite framework vibrations (and therefore not detectable).[21]

On the other hand, bidentate nitrates can be present either as chelating or bridging structures, involving one or two Cu^{II} ions, respectively (left and middle structures in Scheme 2). The symmetry of the NO_3^- ligand in these structures is identical, resulting in one stretching vibration of the N=O group ($v_{N=O}$), and two modes for the O-N-O group (v_{symNO2} and v_{asNO2}) binding one or two Cu^{II} ions. The latter both fall again in the frequency region of the intense framework vibrations (below 1300 cm^{-1}). Our study can thus only focus on the $v_{N=O}$ vibrations of the bidentate nitrates, which is generally ascribed to bridging structures in the 1650-1600 cm^{-1} range and to the chelating ones at 1585-1500 cm^{-1}.[19b, 20, 22] This assignment has been recently discussed on the basis of theoretical calculations, proposing a higher frequency for the chelating structures with respect to bridging ones, in relation to a more strained O-N-O angle and shorter N=O distance in the former.[23] This implies that the $v_{N=O}$ frequency alone cannot be used to discriminate between the two bidentate structures involving one or two Cu^{II} ions.

Recently, spectra obtained upon interaction of NO/O$_2$ (or NO$_2$ alone) at 200 °C on a zeolite similar in composition to CHA15_05, were assigned to bidentate chelating nitrates.[4b, 14] The assignment was based on EXAFS evidences, pointing to the presence of multiple scattering paths in the coordination sphere of Cu, compatible with the Cu-bidentate nitrate geometry (linear arrangement of Cu – N- O atoms, see Scheme 2). Moreover, Cu-Cu pairs at short distance could not be detected, which would be necessary for the formation of bridging structures (*ca* 3 Å, middle structure in Scheme 2).[4b] Our data do not contradict this interpretation. Indeed, the presence of Cu-Cu pairs is statistically favoured at high Cu loadings and low Si/Al, so that it is highly unlikely on sample CHA29_06 (Si/Al = 29). This zeolite shows a relatively high intensity of the three components (azure curve in Figure 6), so that we can safely discard the assignment of one of these to bridging bidentate nitrates. Moreover, no evidence for the band at 1625 cm^{-1} (traditionally assigned to bridging bidentate structures)[15] is observed on CHA5_01 zeolite (blue curve), where the high Al content (Si/Al = 5) should favour the presence of Cu-Cu pairs.

We found further support to this interpretation on the basis of what proposed by Hadjiivanov[22a] and Venkov,[24] who showed the possibility to discriminate between the two very similar bidentate structures by analysis of the nitrates overtone and combination modes. More precisely, they assigned a band around 2620 cm^{-1} to the combination mode of bridged nitrates ($v_{asNO2}+v_{N=O}$) and one around 2580 cm^{-1} to that of chelating ones. In our work, in all zeolites, only a single weak band was observed at 2590 cm^{-1}, developing in parallel with the main $Cu^{II}NO_3^-$ peaks, supporting the absence of bridging structures in all zeolites (Figure 7).
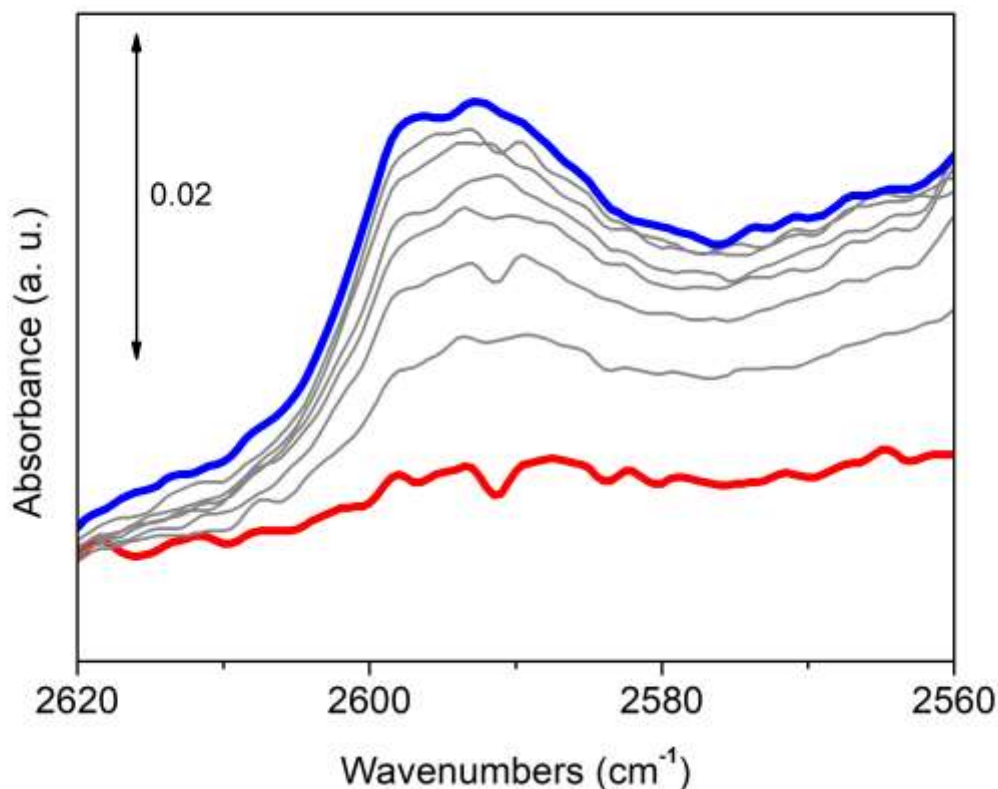
Figure 7. FTIR spectra in the combination mode region of nitrates, measured during exposure of Cu-CHA (Si/Al = 15, Cu/Al 0.5, 2.6 wt% Cu) to 1000 ppm NO/ 10% O_2 at 200°C after initial heating in O_2 at 400°C – red curve after 3 minutes, blue curve after 30 minutes, grey for intermediate time.

Thus, the three bands at 1625, 1610 and 1575 cm^{-1} need to be related to the $\nu_{N=O}$ vibration of different families of bidentate chelating nitrates (left hand structure in Scheme 2). A careful analysis of the three components intensity evolution in different experiments was carried out (see Figure S2 in SI for one example), evidencing that the components at 1610 and 1575 cm^{-1} always go together, at variance with the one at 1625 cm^{-1}, as also evidenced by the results described above. Moreover, the spectral shape observed in all experiments clearly show a peculiar constancy in the 'hole' between the bands at 1610 and 1575 cm^{-1} (1585 cm^{-1}, indicated by § in Figure 6). This is a typical shape of derivative spectra, often observed in the presence of resonance phenomena between vibrational modes of the same molecular groups, as observed for the AB diad of νOH ($_{zeolite}$O-H$\cdots$O$_{water}$) mode described above.[17] However, isotopic exchange experiments with both D_2O and ^{15}NO (not reported, see for instance Chen et al. for results with ^{15}NO and $^{18}O_2$)[15], allowed us to exclude a resonance effect involving $\delta NO_3^-/\delta$OH modes. On the other hand, this spectral shape is characteristic of nitrate on zeolites,[13b, 13d, 13e, 15, 16c, 25] while it is not observed on other oxides.[26] We thus put forward the hypothesis that the two bands centred at 1610 and 1575 cm^{-1} are related to a single chelating nitrate.

On the basis of the above considerations, we need to interpret the spectroscopic features formed in the presence of NO/O_2 in the 1750-1500 cm^{-1} range in terms of two distinct chelating nitrates, structurally similar the left hand one of Scheme 2. The clear differences among samples with different composition (Figure 6) could be thus interpreted in terms of Z-[Cu(OH)]^{I} and Z$_2$-Cu^{II} sites, whose expected relative amount is listed in Table 1. Based on this, CHA5_01 (Si/Al = 5) should mainly present Z$_2$-Cu^{II} sites, which are instead highly unlikely in CHA29_06, where Z-[Cu(OH)]^{I} are favoured due to the very high Al dilution (Si/Al = 29). As already discussed, in the former only two weak low frequency components can be observed, while all bands are intense and well defined in the latter

(compare blue and azure curves in Figure 6). This implies that the spectroscopic multiplicity of chelating nitrates cannot be ascribed to their involvement of Z-[Cu(OH)]^I and Z$_2$-Cu^{II} sites. An important consequence of this is that nitrates are hardly formed (in the tested conditions) on the sample with the highest concentration of Z$_2$-Cu^{II} sites, indicating that we are mainly probing Z-[Cu(OH)]^I sites (and/or Z-[Cu(O$_2$)]^I sites stabilized by one framework negative charge and including a superoxo ligand)[2b, 11] with different local environment. Indeed, recent results from some of us showed that a small fraction of Z-[Cu(OH)]^I sites is also present on CHA5_01,[9, 27] explaining the presence of the two weak components at 1610/1575 cm^{-1}.

The speciation of Cu sites as a function of activation temperature in inert conditions on the same set of samples studied in this work was recently reported.[9] The use of N$_2$ as probe molecule could discriminate Cu^I sites located in the 6 and 8-member rings (6r and 8r) of the zeolite framework, in agreement with in situ XRD/XANES studies.[27] Interestingly, the relative fraction of Cu^I sites in 6r and 8r was found to be dependent on the Cu/Al and Si/Al ratio of the Cu-CHA zeolites, with a general trend similar to that observed in Figure 6. It would thus be tempting to assign the different $v_{N=O}$ bands to chelating nitrates formed by reaction of NO and O$_2$ with Z-[Cu(OH)]^I sites initially located in 6r and 8r windows. However, this hypothesis has weak points. First, DFT calculations showed an almost identical geometry (including O-N-O bond angles and N=O distance) for chelating nitrates involving Cu^{II} ions in the two chabazite rings.[14] Secondly, similar set of bands have been reported in zeolites with different topologies, such as Cu-BEA[13e, 15] and Fe-MFI.[16c, 25]

These considerations would imply that two structurally identical complexes give a different infrared fingerprint. The only explanation is that one of the nitrate ligands is perturbed, *i.e.* it is feeling a different local environment. For instance, it was shown that the CHA zeolite exposes two families of OH Brønsted sites, with identical acidity when probed with CO, but distinct vOH position, in relation to the protons exposure to the cages.[28] We thus propose that what we observe is a perturbation of the nitrate $v_{N=O}$ mode by the zeolite cage or by the presence of vicinal Brønsted sites. Indeed, if we compare the relative intensity of the bands in samples CHA15_05 and CHA15_02 (same Si/Al ratio but different Cu/Al one, red and orange, respectively) the band at 1625 cm^{-1} is almost identical (small differences could be related to background subtraction procedure), while the components at 1610/1575 cm^{-1} are lower in the sample with higher amount of Brønsted sites. A maximum in the bands intensity is instead observed on sample CHA29_06, where the density of Brønsted sites is lowest. Based on semi-quantitative considerations about the concentration of Cu sites in the samples with different Si/Al ratios, the bands at 1610/1575 cm^{-1} are likely characterized by a higher extinction coefficient with respect to the 1625 cm^{-1} one.

This could explain the relative decrease of the band at 1625 cm^{-1} when the temperature is lowered (Figure 3). Indeed, our results show that reducing the temperature favours the formation of NO$^+$, with parallel water evolution and 1:1 H$_2$O/H$^+$ adduct formation. It is thus reasonable to propose that a nitrate species interacting with vicinal Brønsted sites (inducing a shortening of the N=O bond and/or straining of the O-N-O angle)[23] would be perturbed when H$^+$ are consumed to produce and exchange NO$^+$ ions, and involved in strong hydrogen bonds. This would also explain the absence of the 1625 cm^{-1} band on CHA5_01, where the formation of NO$^+$ and hydrogen bonded 1:1 H$_2$O/H$^+$ adducts is high even at 200 °C. Further studies would be necessary to get a more precise description of the 'perturbed' chelating nitrates by using different techniques and approaches such as *operando* XAS and EPR[29] coupled to DFT calculations.

Implications on the SCR reaction mechanism

The equilibrium between surface $Cu^{II}NO_3^-$ and $Cu^{II}NO_2^-$ has been proposed to be a key step in the NH$_3$-SCR.[4b, 14] However, the recent work by Paolucci et al., showing the mobilization of Cu ions by NH$_3$, pointed to the activation of oxygen by Cu-Cu pairs as rate determining step of the reaction.[4c]

The reported experiments do not include NH_3, so we cannot provide new information about the SCR mechanism. However, we believe that the role of nitrates formation on Cu-zeolites still deserves some understanding, also in relation to the higher rate measured when NO_2 is added to the feed (standard *vs* fast SCR, reactions 1 and 2). Indeed the role of nitrate in the SCR cycle has been recently debated by Marberger et al.[6a] and by Chen et al., who proposed NO^+ as key intermediate in the reaction.[15]

The nitrosonium ion NO^+ has been proposed to be formed by the reaction of NO (in the presence of oxygen) with the zeolite Brønsted sites.[15-16, 18] According to the mechanisms proposed by Hadjiivanov and by Henriques et al., the reaction involves a transfer of the NO unpaired electron, located on an antibonding π^* orbital, with formation of water.[16a, 16b, 18] In agreement with the proposed reaction mechanisms, our results show a significant formation of NO^+ and hydrogen bonded 1:1 H_2O/H^+ adducts on the sample characterized by the lowest Si/Al ratio (CHA5_01, Si/Al = 5), and a decrease in the other samples roughly proportional to their Brønsted concentration (inset of Figure 6). Moreover, we showed for the first time the effect of temperature on this reaction, which is favoured at 50 °C, and almost negligible (apart for sample CHA5_01) at 200 °C. This sample is also characterized by the highest hydrophilicity, in relation to the high Al content, so that we cannot exclude a role of this parameter in affecting the reaction equilibrium, which could be in competition with the nitrates evolution.

According to the interpretation discussed above, two structurally similar chelating nitrates (left structure in Scheme 2) are formed in most of samples, irrespective of the Cu/Al and Si/Al ratio, and no evidence for bridging complexes (middle structure in Scheme 2) is found even at Si/Al = 5, pointing to the fact that nitrates bridging two Cu^{II} ions are not favoured in this framework. Moreover, we clearly show that nitrate formation is not involving Z_2-Cu^{II} sites, probably in relation to their high stability.[3, 6b, 30] Both observations imply that the coordination of the nitrate ligand to the Cu^{II} ions is not able to mobilize them, at variance with what observed with NH_3.[4b, 4c, 6a, 31]

Coming to the effect of temperature, the increase of nitrate intensity at 50 °C is not surprising, since adsorption is an exothermic phenomenon and nitrates do not show a high thermal stability. Our interpretation of the bands at 1625 cm^{-1} to a chelating nitrate perturbed by the vicinity of Brønsted sites can instead explain the decrease of this component while lowering the temperature, as a side effect of the NO^+ and H_2O/H^+ formation. In the same conditions, monodentate nitrates are also observed on all samples, showing the coexistence of different structures (all involving single Cu^{II} sites) at low temperature. No correlation could be observed between the decrease of the band at 1625 cm^{-1} and the growth of NO^+ or monondentate nitrates, suggesting that these are parallel reactions, at variance with what proposed by Chen et al., who proposed that surface nitrates could block the formation of NO^+.[15]

Finally, our experiments with water in the flow (that is in conditions closer to the exhaust gas mixture in real systems) clearly indicates that water is rapidly physisorbed on Cu^{II} ions at both temperatures (thought with a slower rate at 50°C), replacing the existing chelating nitrates. However, at 50 °C stable monodentate nitrates are formed in the presence of water clusters, and coexist with a fraction of solvated ionic ones. We could hypothesize that (a fraction of) these monodentate species are formed by insertion of one water molecule in the coordination sphere of Cu^{II} ions initially involved in chelating nitrate complexes. However, no correlation was observed with the intensity decrease of the band at 1625 cm^{-1}. The reactivity to NO^+ in the presence of H_2O in the flow does not show a correlation with the nitrate evolution; this species is rapidly depleted already in the presence of hydrogen bonded 1:1 H_2O/H^+ adducts (that is before formation of H_2O clusters).

Conclusions

FTIR spectroscopy was used in *operando* conditions to study the formation of $Cu^{II}(N,O)$ species as a result of NO oxidation with O_2 on a series of Cu-CHA samples with different composition. This allowed us to explain the spectral multiplicity of nitrate bands often observed in transition metal exchanged zeolites, and to definitely exclude the presence of bridging bidentate nitrates (middle structure in Scheme 2), irrespective of the Si/Al and Cu loadings. Chelating nitrates could be formed both at 200 and 50 °C, with different concentration which can be ascribed to their thermal stability and to the concomitant presence of competitive reactions. Namely, NO^+ (if formed) was found to be unstable at 200 °C on most of the samples and inhibited by the formation of hydrogen bonded 1:1 H_2O/H^+ adducts. The concentration of this ion was found to be in good correlation with the Brønsted concentration of the Cu-CHA zeolites, in agreement with the proposed mechanism involving H+ sites. On the other hand, monodentate nitrates (right structure in Scheme 2) were favoured by low temperature and by the presence of water (both involved in 1:1 adducts with Brønsted sites and in molecular clusters). Finally, we showed that nitrates are not formed on Z_2-Cu^{II} sites, in relation to their strong interaction with the framework, while Z-$[Cu(OH)]^+$ and Z-$[Cu(O_2)]^+$ ions are likely involved in this reactivity.

Experimental Section

Sample preparation

CHA sample with Si/Al of 15 and 29 are prepared tuning suitably the synthesis gel composition (1.0 SiO_2/0.033 Al_2O_3/0.5 TMAdaOH/0.5 HF/3 H_2O). The gel is prepared by dissolving aluminum isopropoxide (98%, Sigma-Aldrich) in tetraethyl orthosilicate (98% Aldrich) and adding N,N,Ntrimethyladamantammonium hydroxide (TMAdaOH, 25 wt %,Sachem) to the solution. This mixture is then stirred to homogenize and hydrofluoric acid (48 wt %, 99.99% trace-metal basis, Sigma-Aldrich) is added; the mixture is then dried at 60°C and stirred by hand and until the desired water content is obtained. Subsequently, the gel is heated to 150 °C for 3 days under rotation in a Teflon-lined autoclave. The CHA product is recovered by filtration, washed several times with water and calcined at 580 °C for 3 h to remove the TMAdaOH.

CHA zeolite with Si/Al 5 is synthesized mixing 32.9 g of de-ionized water with 13.4g of N,N,N-trimethyl-1-adamantanamine hydroxide(TMAdaOH, 25 wt %, Sachem Inc.) and 0.2 g of sodium hydroxide (Sigma-Aldrich, > 98.0%); subsequently 20 g of sodium silicate solution (26.5 wt % SiO2, Sigma Aldrich) and 2 g of USY (CBV 500) are added. The so-obtained mixture is then placed in a Teflon lined autoclave under rotation and crystallized for 6 days in a pre-heated oven (140 °C). The product is again filtered and washed with de-ionized water and dried at 105 °C overnight. The zeolite is calcined at 580 °C to remove the templating agent and the calcined product is ion-exchanged (3 × 2 hours at 80°C) with ammonium using 1 M ammonium nitrate solution, followed by a calcination at 500 °so to have the proton form of the zeolite.

To prepare the corresponding Cu-CHA zeolites, the required amount of copper(II) acetate monohydrate (Sigma-Aldrich, 99.99%) is dissolved in water and the proton form of the zeolite is added to the solution (250 ml per zeolite gram). The solution is stirred at room temperature for 24h and then the obtained copper zeolite is filtered, washed, dried at 100°C overnight then it is calcined at 500°C for 3 hours to remove the residual acetate.

Fourier transform infrared spectroscopy (FTIR)

FTIR spectra in *operando* conditions were recorded in transmission mode on a PerkinElmer System 2000 infrared spectrophotometer, equipped with a MCT detector; 128 interferograms (recorded at 2 cm^{-1} resolution) were typically averaged for each spectrum. Zeolites powders were pressed in form

of self-supporting pellets of ca. 15 mg and placed inside a commercial FTIR reactor cell (AABSPEC, no. 2000-A multimode) with controlled gas atmosphere and temperature. The gas flow used in the experiments was 50 ml/min. All measured catalysts were first treated in O_2 at 400 °C for 60 min (heating rate 5 °C min^{-1}), then cooled to 200 °C or to 50°C (cooling rate 3°C min^{-1}) in O_2 and exposed to a mixture of 1000 ppm NO and 10% O_2 in N_2. When working in wet conditions, 5% H_2O was dosed on the zeolite, with N_2 as vapour carrier.
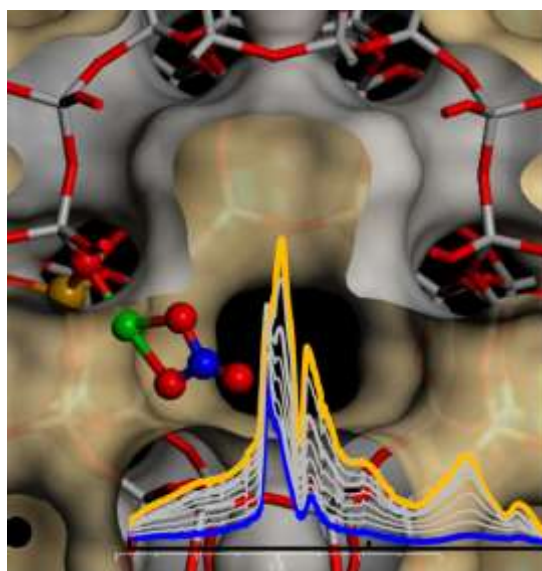
Keywords

SCR, Cu-CHA, NO oxidation, FTIR, nitrates, operando spectroscopy

Graphical abstract

References

[1]   A. M. Beale, F. Gao, I. Lezcano-Gonzalez, C. H. F. Peden, J. Szanyi, *Chem Soc Rev* **2015**, *44*, 7371-7405.
[2]   a) M. J. Wulfers, S. Teketel, B. Ipek, R. F. Lobo, *Chem Commun* **2015**, *51*, 4447-4450; b) D. K. Pappas, E. Borfecchia, M. Dyballa , I. A. Pankin, K. A. Lomachenko, A. Martini, M. Signorile, S. Teketel, B. Arstad, G. Berlier, C. Lamberti, S. Bordiga, U. Olsbye, K. P. Lillerud, S. Svelle, P. Beato, *J Am Chem Soc* **2017**, *139*, 14961-14975; cR. Oord, J. E. Schmidt, B. M. Weckhuysen, *Catal Sci Technol* **2018**, *8*, 1028-1038.
[3]   E. Borfecchia, K. A. Lomachenko, F. Giordanino, H. Falsig, P. Beato, A. V. Soldatov, S. Bordiga, C. Lamberti, *Chem Sci* **2015**, *6*, 548-563.
[4]   a) S. Kieger, G. Delahay, B. Coq, B. Neveu, *J Catal* **1999**, *183*, 267-280; b) T. V. W. Janssens, H. Falsig, L. F. Lundegaard, P. N. R. Vennestrom, S. B. Rasmussen, P. G. Moses, F. Giordanino, E. Borfecchia, K. A. Lomachenko, C. Lamberti, S. Bordiga, A. Godiksen, S. Mossin, P. Beato, *ACS Catal* **2015**, *5*, 2832-2845; c) C. Paolucci, I. Khurana, A. A. Parekh, S. C. Li, A. J. Shih, H. Li, J. R. Di Iorio, J. D. Albarracin-Caballero, A. Yezerets, J. T. Miller, W. N. Delgass, F. H. Ribeiro, W. F. Schneider, R. Gounder, *Science*

2017, *357*, 898; d) C. Paolucci, A. A. Verma, S. A. Bates, V. F. Kispersky, J. T. Miller, R. Gounder, W. N. Delgass, F. H. Ribeiro, W. F. Schneider, *Angew. Chem.-Int. Edit.* **2014**, *53*, 11828-11833.

[5]   F. Gao, D. H. Mei, Y. L. Wang, J. Szanyi, C. H. F. Peden, *J Am Chem Soc* **2017**, *139*, 4935-4942.

[6]   a) A. Marberger, A. W. Petrov, P. Steiger, M. Elsener, O. Krocher, M. Nachtegaal, D. Ferri, *Nat. Catal.* **2018**, *1*, 221-227; b) C. Paolucci, A. A. Parekh, I. Khurana, J. R. Di Iorio, H. Li, J. D. A. Caballero, A. J. Shih, T. Anggara, W. N. Delgass, J. T. Miller, F. H. Ribeiro, R. Gounder, W. F. Schneider, *J Am Chem Soc* **2016**, *138*, 6028-6048.

[7]   a) L. Chen, H. Falsig, T. V. W. Janssens, H. Gronbeck, *J Catal* **2018**, *358*, 179-186; b) H. Falsig, P. N. R. Vennestrom, P. G. Moses, T. V. W. Janssens, *Topics in Catalysis* **2016**, *59*, 861-865.

[8]   L. Chen, H. Falsig, T. V. W. Janssens, J. Jansson, M. Skoglundh, H. Gronbeck, *Catal Sci Technol* **2018**, *8*, 2131-2136.

[9]   A. Martini, E. Borfecchia, K. A. Lomachenko, I. A. Pankin, C. Negri, G. Berlier, P. Beato, H. Falsig, S. Bordiga, C. Lamberti, *Chem Sci* **2017**, *8*, 6836-6851.

[10]   F. Giordanino, P. N. R. Vennestrom, L. F. Lundegaard, F. N. Stappen, S. Mossin, P. Beato, S. Bordiga, C. Lamberti, *Dalton T* **2013**, *42*, 12741-12761.

[11]   A. Martini, E. Alladio, E. Borfecchia, *Topics in Catalysis* **2018**, *accepted*.

[12]   a) F. Gao, J. H. Kwak, J. Szanyi, C. H. F. Peden, *Topics in Catalysis* **2013**, *56*, 1441-1459; b) F. Gao, E. D. Walter, M. Kollar, Y. L. Wang, J. Szanyi, C. H. F. Peden, *J Catal* **2014**, *319*, 1-14; c) K. A. Lomachenko, E. Borfecchia, C. Negri, G. Berlier, C. Lamberti, P. Beato, H. Falsig, S. Bordiga, *J Am Chem Soc* **2016**, *138*, 12025-12028.

[13]   a) T. Selleri, M. P. Ruggeri, I. Nova, E. Tronconi, *Topics in Catalysis* **2016**, *59*, 678-685; b) M. P. Ruggeri, I. Nova, E. Tronconi, J. A. Pihl, T. J. Toops, W. P. Partridge, *Appl Catal B-Environ* **2015**, *166*, 181-192; c) M. Colombo, I. Nova, E. Tronconi, *Catal Today* **2012**, *197*, 243-255; d) J. Szanyi, J. H. Kwak, H. Y. Zhu, C. H. F. Peden, *Phys Chem Chem Phys* **2013**, *15*, 2368-2380; eH. Y. Chen, Z. H. Wei, M. Kollar, F. Gao, Y. L. Wang, J. Szanyi, C. H. F. Peden, *Catal Today* **2016**, *267*, 17-27.

[14]   C. Tyrsted, E. Borfecchia, G. Berlier, K. A. Lomachenko, C. Lamberti, S. Bordiga, P. N. R. Vennestrom, T. V. W. Janssens, H. Falsig, P. Beato, A. Puig-Molina, *Catal Sci Technol* **2016**, *6*, 8314-8324.

[15]   H.-Y. Chen, M. Kollar, Z. Wei, F. Gao, Y. Wang, J. Szanyi, C. H. F. Peden, *Catal Today* **2018**.

[16]   a) K. Hadjiivanov, J. Saussey, J. L. Freysz, J. C. Lavalley, *Catal Lett* **1998**, *52*, 103-108; b) C. Henriques, O. Marie, F. Thibault-Starzyk, J. C. Lavalley, *Micropor Mesopor Mat* **2001**, *50*, 167-171; c) M. Rivallan, G. Ricchiardi, S. Bordiga, A. Zecchina, *J Catal* **2009**, *264*, 104-116.

[17]   a) S. Bordiga, L. Regli, C. Lamberti, A. Zecchina, M. Bjorgen, K. P. Lillerud, *J Phys Chem B* **2005**, *109*, 7724-7732; b) C. Paze, S. Bordiga, C. Lamberti, M. Salvalaggio, A. Zecchina, G. Bellussi, *J Phys Chem B* **1997**, *101*, 4740-4751.

[18]   A. W. Aylor, L. J. Lobree, J. A. Reimer, A. T. Bell, *J Catal* **1997**, *170*, 390-401.

[19]   a) T. M. Miller, V. H. Grassian, *Geophys Res Lett* **1998**, *25*, 3835-3838; b) J. Szanyi, J. H. Kwak, R. J. Chimentao, C. H. F. Peden, *J Phys Chem C* **2007**, *111*, 2661-2669; c) B. Djonev, B. Tsyntsarski, D. Klissurski, K. Hadjiivanov, *J Chem Soc Faraday T* **1997**, *93*, 4055-4063.

[20]   K. I. Hadjiivanov, *Catal Rev* **2000**, *42*, 71-144.

[21]   B. O. Field, C. J. Hardy, *Journal of the Chemical Society* **1963**, 4428 - 4434.

[22]   a) K. Hadjiivanov, *Catal Lett* **2000**, *68*, 157-161; bC. Borensen, U. Kirchner, V. Scheer, R. Vogt, R. Zellner, *J Phys Chem A* **2000**, *104*, 5036-5045.

[23]   L. Tribe, R. Hinrichs, J. D. Kubicki, *J Phys Chem B* **2012**, *116*, 11266-11273.

[24]   T. Venkov, K. Hadjiivanov, D. Klissurski, *Phys Chem Chem Phys* **2002**, *4*, 2443-2448.

[25]   a) Q. Sun, Z. X. Gao, H. Y. Chen, W. M. H. Sachtler, *J Catal* **2001**, *201*, 89-99; b) M. Devadas, O. Krocher, M. Elsener, A. Wokaun, G. Mitrikas, N. Soger, M. Pfeifer, Y. Demel, L. Mussmann, *Catal Today* **2007**, *119*, 137-144.

[26]   a) S. Morandi, F. Prinetto, G. Ghiotti, M. Livi, A. Vaccari, *Micropor Mesopor Mat* **2008**, *107*, 31-38; b) S. Morandi, F. Prinetto, L. Castoldi, L. Lietti, P. Forzatti, G. Ghiotti, *Phys Chem Chem Phys* **2013**, *15*, 13409-13417; c) L. Cao, L. Chen, X. D. Wu, R. Ran, T. F. Xu, Z. Chen, D. Weng, *Appl. Catal. A-Gen.* **2018**, *557*, 46-54.

[27] C. W. Andersen, E. Borfecchia, M. Bremholm, M. R. V. Jorgensen, P. N. R. Vennestrom, C. Lamberti, L. F. Lundegaard, B. B. Iversen, *Angew. Chem.-Int. Edit.* **2017**, *56*, 10367-10372.

[28] S. Bordiga, L. Regli, D. Cocina, C. Lamberti, M. Bjorgen, K. P. Lillerud, *J Phys Chem B* **2005**, *109*, 2779-2784.

[29] a) I. Ellmers, R. P. Velez, U. Bentrup, A. Bruckner, W. Grunert, *J Catal* **2014**, *311*, 199-211; b) I. Ellmers, R. P. Velez, U. Bentrup, W. Schwieger, A. Bruckner, W. Grunert, *Catal Today* **2015**, *258*, 337-346; c) R. P. Velez, I. Ellmers, H. M. Huang, U. Bentrup, V. Schunemann, W. Grunert, A. Bruckner, *J Catal* **2014**, *316*, 103-111.

[30] A. Godiksen, F. N. Stappen, P. N. R. Vennestrom, F. Giordanino, S. B. Rasmussen, L. F. Lundegaard, S. Mossin, *J Phys Chem C* **2014**, *118*, 23126-23138.

[31] F. Giordanino, E. Borfecchia, K. A. Lomachenko, A. Lazzarini, G. Agostini, E. Gallo, A. V. Soldatov, P. Beato, S. Bordiga, C. Lamberti, *J Phys Chem Lett* **2014**, *5*, 1552-1559.